NJC

Accepted Manuscript

This article can be cited before page numbers have been issued, to do this please use: S. Li, L. Sun, J. C. Ni, Z. Shi, Y. H. Xing, D. Shang and F. Bai, *New J. Chem.*, 2017, DOI: 10.1039/C6NJ03933B.

ROYAL SOCIETY OF CHEMISTRY

rsc.li/njc

View Article Online
DOI: 10.1039/C6NJ03933B

Journal Name

ARTICLE

Two Uranyl Heterocyclic Carboxyl Compounds with Fluorescent Properties as High Sensitivity and Selectivity Optical Detectors for Nitroaromatics

Received 00th January 20xx,
Accepted 00th January 20xx

DOI: 10.1039/x0xx00000x

www.rsc.org/

Shuang Li,[a] Li Xian Sun,[b] Jue Chen Ni,[a] Zhan Shi,[c] Yong Heng Xing,*[a] Di Shang,[a] Feng Ying Bai*[a]

ABSTRACT: The two compounds, $UO_2(C_{16}H_7N_4O_4)_2{\cdot}2H_2O$ (**1**) and $UO_2(C_{20}H_{12}N_5O_2)_2$ (**2**) have been synthesized, based on the different heterocyclic carboxyl ligands, 2,3-pyrazino[1,10]phenanthroline-2,3-dicarboxylic acid (H_2L_1) and 2,6-bis(2-pyrazinyl)pyridine-4-benzoic acid (HL_2). Two compounds were characterized by the elemental analysis, IR spectroscopy, PXRD, thermogravimetric analysis and UV-vis Spectroscopy. The single crystal X-ray diffraction analysis revealed that both compounds **1** and **2** exhibited 2D sheet structures. Moreover, the study of fluorescence quenching properties of compounds **1** and **2** showed that the luminescent intensity decrease for both **1** and **2** were especially obvious with the increasing of the nitroaromatics concentration, even if the nitroaromatics were at a very low concentration (for **1** is 15 ppm, for **2** is 20 ppm), which can also be detected. The experimental results suggest a high selective quenching of initial fluorescence intensity in the presence of nitroaromatic compounds. And by calculating the quenching constants of the nitroaromatics using the SV equation $(I_0/I) = K_{SV}[A] + 1$, we can see the K_{SV} values of the quencher TNP are both largest for two compounds, and the values are 1.6×10^6 and 8.5×10^5 for **1** and **2**, respectively. It means that the two compounds are of the best sensitive luminescence. In addition, compound **2** exhibit enhanced fluorescence behavior towards to aldehyde compounds, showing a turn-on fluorescence responsive behavior.

Introduction

The rapid and selective detection of high energetic chemicals have become a major concern, which due to the increasing use of explosive materials.[1-4] Therefore, the development of simple, inexpensive and rapid detection methods of trace explosive materials has become very important, that is mainly applied in the fields of homeland security, environmental implications and so on.[3b,5-7] As we known, nitroaromatics, one of the most important chemical intermediates, have been widely used for dye, pharmaceuticals, fluorescent probes and pesticide in recent years.[8] Moreover, nitroaromatics remain as key energetic materials for the preparation of landmines and improvised explosive devices (IED).[5a] Nitroaromatics include 2,4,6-trinitrophenol (TNP), 2,4,6-trinitrotoluene (TNT), 2,4,6-trinitrobenzene (TNB), 2,4-dinitrotoluene (DNT), and 1,3-dinitrobenzene (DNB), etc., which are the main ingredients of explosives, and they also are classified as plastic explosives.[9,10] Among all of the nitroaromatics, 2,4,6-trinitrophenol (TNP) is one of the most dangerous chemicals and its explosive nature is even stronger than 2,4,6-trinitrotoluene (TNT), and TNP has been used as an important ingredient of explosives and rocket fuels.[8b,11,12] Beside these, TNP is used in glass, match, fireworks, dye, and lather industries.[8c] However, the nitroaromatics are well-known as the highly toxic contaminant with broad range of detriment, and TNP also causes unpleasant effects on human health such as irritant to skin/eye and damage the respiratory system.[11b,13] Moreover, aldehydes are great harm for our health. Therefore, the highly sensitive and selective detection of nitroaromatics and aldehydes are of high significance. Up to now, many methods have been reported, such as canines and sophisticated instrumental methods, for nitroaromatics detection are inconvenient and not always available.[14] And as we known, fluorescence sensing is the change of the interaction between the molecules and the fluorescence signal; the aim is to achieve special recognition of certain molecules or ions. The fluorescence signals are including fluorescence enhancement or quenching, the change of fluorescence characteristic peak position, change of fluorescence lifetime and change of fluorescence polarization, and so on. Thus, to solve these problems, optical detection method is attracting increasing attention because of their high simplicity, sensitivity and quick response time, and the design of coordination polymers/metal–organic

[a] College of Chemistry and Chemical Engineering, Liaoning Normal University, Huanghe Road 850#, Dalian 116029, P.R. China.
E-mail: xingyongheng2000@163.com, baifengying2000@163.com
[b] Guangxi Key Laboratory of Information Materials, Guilin University of Electronic Technology, Guilin 541004, P.R. China.
[c] State Key Laboratory of Inorganic Synthesis and Preparative Chemistry, College of Chemistry, Jilin University, Changchun 130012, P.R. China.

† Electronic supplementary information (ESI) available: Figures of Infrared spectra, figure of structure, TG analyses, PXRD, UV-vis Spectroscopy, band gap and the bond lengths (Å) and angles (°) are presented in the supplementary material. CCDC 1491331-1491332. See DOI: 10.1039/x0xx00000x

View Article Online
DOI: 10.1039/C6NJ03933B

frameworks based luminescence detectors for nitro explosives has been developing rapidly.[15,16] Compared with the huge amount of 3d and 4f metal–organic frameworks, 5f actinide compounds that adopt more various topologies and coordination geometries have been less investigated. Recently, the chemistry of actinide mixed materials has attracted more and more attention. Moreover, uranyl–organic assemblies have received considerable attention not only due to the diverse chemical compositions and architectures, but also have a wide range of important physicochemical properties that include ion exchange, ionic conductivity, intercalation chemistry, photochemistry, nonlinear optics, selective oxidation catalysis and so on.[17-19] In the past literatures, we could see that, the uranium metals always coordinated with oxygen atoms from the ligands.[20] And the uranium exhibits an interesting chemical ability to successfully form an abundant variety of frameworks with different network dimensionalities through 4–6 additional coordination sites in the equatorial plane (4+2, square bipyramid; 5+2, pentagonal bipyramid; 6+2, hexagonal bipyramid), and the central metal uranium coordinated with the nitrogen atoms (N) from the N-heterocyclic ligands makes the compound structures and properties more abundant.[21]

Herein, we have utilized two different heterocyclic carboxyl ligands, 2,3-pyrazino[1,10]phenanthroline-2,3-dicarboxylic acid (H_2L_1) and 2,6-bis(2-pyrazinyl)pyridine-4-benzoic acid (HL_2), the molecular structures are shown in the Scheme 1, to react with $UO_2(CH_3COO)_2{\cdot}2H_2O$, and constructed two the new compounds, $UO_2(C_{16}H_7N_4O_4)_2{\cdot}2H_2O$ (**1**) and $UO_2(C_{20}N_5O_2H_{12})_2$ (**2**) under the hydrothermal condition, respectively. The two compounds were characterized by single-crystal X-ray diffraction, IR spectra, UV-vis spectra, XRD analysis and the thermal properties. What's more, we have researched the mechanism of quenching mechanism, selectivity and sensitivity of different nitroaromatics through the two compounds as substrates in detail.

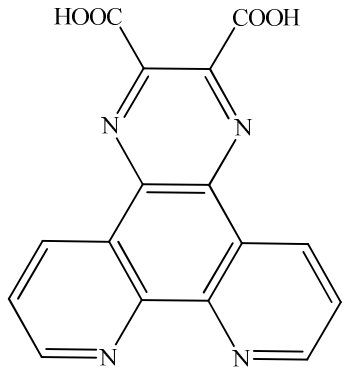

(a)

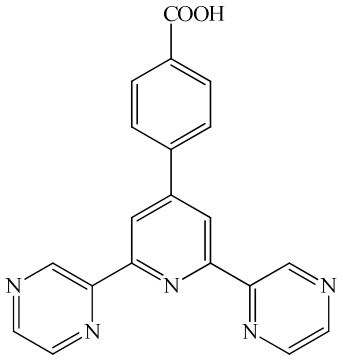

(b)

Scheme 1. The molecular structures of (a): H_2L_1, (b): HL_2.

Experimental

Caution! While all the uranyl compounds used in these studies contained depleted uranium salts, standard precautions were performed for handling radioactive materials, and all studies were conducted in a laboratory dedicated to studies on actinide elements.

Materials and Methods. All chemicals purchased commercially were of reagent grade or better and used without further purification (Sinopharm Chemical Reagent Co., Ltd.). Elemental analyses of C, H, and N were conducted on a Perkin-Elmer 240C automatic analyzer at the analysis center of Liaoning Normal University. All IR measurements were obtained using a Bruker AXS TENSOR-27 FT-IR spectrometer with pressed KBr pellets in the range of 400–4000 cm^{-1} at room temperature. UV-vis-NIR spectra for two compounds, and the ligands (H_2L_1 and HL_2) were recorded on a JASCO V-570 UV/VIS/NIR microspectrophotometer (200-2500 nm, in the form of solid sample). Thermogravimetric analysis (TG) was performed on a Perkin Elmer Diamond TG/DTA under the conditions of the N_2 atmosphere in the temperature range from 30 to 1000 °C. X-ray powder diffraction patterns were obtained on a Bruker Advance-D8 equipped with Cu Ka radiation, in the range 5° < 2θ < 55°, with a step size of 0.02° (2θ) and an count time of 2s per step. The photoluminescent properties of the compounds **1** and **2** were measured in the solid state and in different solvent emulsions on a JASCO FP-6500 spectrofluorimeter at room temperature. The electrode is made of optical glass coated with indium and tin oxides (ITO). Standard p-type silicon flakes were used to adjust the comparative phase, and a xenon lamp was used as an Illuminator to supply radiation in the range of 300–800 nm.

Synthesis

The ligand HL_2 (HL_2= [2,6-bis(2-pyrazinyl)pyridine-4-benzoic acid]) was synthesized according to the method described in the literature.[22] The solution of 2.0 mol/L sodium hydroxide (50 ml) was added into the mixing solution of acetylpyrazine (3.260 g, 26.7 mmol) and 4-Carboxybenzaldehyde (4.035 g, 26.7 mmol) in the 50ml ethanol at 0–5 °C under stirring by dropwise. Then, the mixture continued to react for 2 h at 0–5 °C, then added

View Article Online
DOI: 10.1039/C6NJ03933B

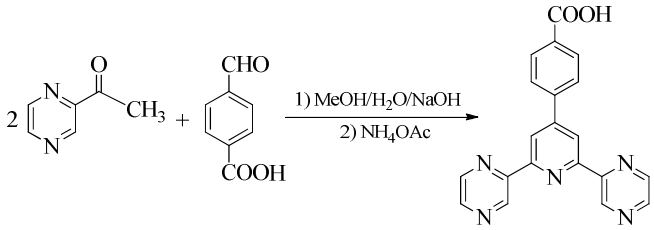

Scheme 2. The ligand HL_2 synthesis process.

acetylpyrazine (3.260 g， 26.7 mmol) and ammonium acetate (10 g, 129.7 mmol) to continue reaction. The mixture was heated to reflux at 100 °C for another 3 h. After cooling to room temperature, the white solid was collected by filtration, then, the white powder was recrystallized with ethanol and filtration. The yield of the product was 65%. The ligand HL_2 synthesis process was shown in the Scheme 2. IR data (KBr, cm^{-1}): 3408(s, br), 3216(s), 1708(m), 1597(s), 1566(s), 1404(w), 1273(s), 1161(w), 1120(w), 1060(m), 1029(m), 898(m), 848(m), 787(w), 706(w), 574(w), 473(w). And the IR spectrum was shown in the Figure S1.

$UO_2(HL_1)_2\cdot 2H_2O$ (**1**) ($L_1=C_{16}N_4O_4H_6$). Compound **1** was synthesized from combining $UO_2(CH_3COO)_2\cdot 2H_2O$ (0.042 g, 0.100 mmol), H_2L_1 (0.008 g, 0.025 mmol), demineralized water (6 mL) and ethanol (3 ml) in glass vessel and stirred for 4 h at room temperature. The yellow suspension with a pH of 4 was put in a 23 mL Teflon-lined stainless steel autoclave and heated statically at 120 °C for 3 days, then allowed to crystallize over 2 days at room temperature. Yellow single crystals were obtained from the resulting solution, which could be isolated with a yield of 45% based on $[UO_2]^{2+}$ after filtration and washing thoroughly with distilled water. Elemental Analysis (%) Calcd for compound **1**, $C_{32}H_{18}N_8O_{12}U$: C, 40.65; H, 1.91; N, 11.86. Found: C, 40.53; H, 1.78; N, 11.86. IR data (KBr, cm^{-1}): 3401(m, br), 2923(w), 2853(w), 1744(w), 1605(s), 1530(w), 1417(m), 1362(m), 1271(w), 1208(w), 928(s), 646(w), 544(w).

$UO_2(L_2)_2$ (**2**) ($L_2=C_{20}N_5O_2H_{12}$). The synthesis of compound **2** was similar to that of **1**, the only difference was that the ligand HL_2 (0.008 g, 0.0230 mmol) was in place of H_2L_1. And yellow single crystals were obtained from the resulting solution, which could be isolated with a yield of 43% based on $[UO_2]^{2+}$ after filtration and washing thoroughly with distilled water. Elemental Analysis (%) Calcd for compound **2**, $C_{40}H_{24}N_{10}O_6U$: C, 49.04; H, 2.45; N, 14.30. Found: C, 48.91; H, 2.37; N, 14.41. IR data (KBr, cm^{-1}): 3471(w, br), 3072w), 1815(m), 1712(w), 1595(m), 1522(m), 1435(s), 1131(m), 1021(m), 919(s), 849(w), 722(w), 480(w).

RESULTS AND DISCUSSION

X-ray Crystal Structure Determination and Structural Descriptions.

Single crystals of suitable dimensions for compounds **1** and **2** were mounted on glass fibers for the X-ray structure determinations. Reflection data were collected at room temperature on a Bruker AXS SMART APEX II CCD diffractometer with graphite monochromatized Mo Kα radiation (λ = 0.71073 Å). A semiempirical absorption correction was applied by the program SADABS.[23] The program suite was used for space-group determination (XPREP), direct method structure solution (XS), and least-squares refinement (XL).[24] Crystal data and structure refinement parameters are given in Table 1, the main selected bond lengths and angles of compounds **1** and **2** are listed in the Table S1.

$UO_2(HL_1)_2\cdot 2H_2O$ (**1**) ($L_1=C_{16}N_4O_4H_6$). As illustrated in Figure 1a, the asymmetric unit in compound **1** consists of one crystallographically independent one uranyl ion, one incompletely deprotonated ligand and one aqua ligand. The uranyl oxygen atom at the apexes are bonded to the central uranium atom (U1) at the distance of 1.760(3) Å and the O=U=O bond angles is 179.99(2)° to form the near-linear $[UO_2]^{2+}$ cation, in good agreement with the reported average uranyl bond length and angle.[25] Six equatorial positions of U1 are occupied by oxygen atoms from three chelating carboxylate groups pertaining to three ligands from different directions. As described above, the whole ligand acts as a μ_3-bridge linking two U^{VI} centers as illustrated in Figure 1b. And the N3 has been protonated in this structure. Intriguingly, the adjacent uranyl polyhedra are linked by carboxyl groups of H_2L_1 ligand to form secondary building units (Figure 1c) and further form infinite one dimensional chains by the ring of the ligand (Figure 1d). The inorganic chains linked by the hydrogen bonds of C1-H1···O4A and N3-H3A···O2 to furthermore form a 2D network structure of compound **1** (Figure 1e), and the hydrogen bonds of O5-H5···O1 make the 2D structure more stable.

$UO_2(L_2)_2$ (**2**) ($L_2=C_{20}N_5O_2H_{12}$). The structure of **2** comprises one crystallographically distinct U^{VI} center and one ligand (HL_2) in the Figure 2a. The uranium atom is eight-coordinated by two atoms with an O=U=O angle of 180.0° and a bond length of 1.746(3) Å, four oxygen atoms from the carboxyl group of two ligands with the bond distances in the range of 2.440(3) Å to 2.474(3) Å, respectively, and two nitrogen atoms from the two ligands with the bond length of 2.699(3) Å, forming a distorted hexagonal bipyramid geometry. As shown in the Figure 2b, two coordination modes of the carboxylate groups in the ligand are observed: chelating bidentate (μ_1-$\eta^1\eta^1$) and monodentate (μ_1-η_N^1). In the extended configuration, each building block $[UO_2(COO)_2N_2]$ connects with four ligands HL_2, in the meantime, each ligand is connected with the two building blocks, to form a two-dimensional structure. As shown in the Figure S2, the hydrogen bonds of C4-H4···N3 make the 2D structure more stable.

Infrared Spectroscopy.

The IR spectra of compounds **1** and **2** were shown in Figure S3. The broad absorption bands appearing at 3401 cm^{-1} of compound **1** indicates the presence of water molecules (for **2**, at 3470 cm^{-1} maybe hydroxy peak of ethanol). For **1**, the peak around 2923 cm^{-1} is attributed to the $-CH_2-$ stretching mode (for **2** at 3072 cm^{-1}). Absorption at 1605, 1417 cm^{-1} of **1** and 1595, 1435 cm^{-1} of **2** are assigned to the asymmetrical stretching vibration and symmetrical stretching vibration of C=O bond, respectively. The bands between 1400–1600 cm^{-1} are attributed to the skeletal vibrations of the organic aromatic rings. And for **1**, the symmetric and asymmetric stretching modes of U=O is observed at about 928 cm^{-1} (919 cm^{-1} for **2**).

View Article Online
DOI: 10.1039/C6NJ03933B

Table 1. Summary of crystal data and refinement results for compounds **1** and **2***

	1	2
Chemical formula	$C_{32}H_{18}N_8O_{12}U$	$C_{40}H_{24}N_{10}O_6U$
M(g mol^{-1})	944.57	978.72
Crystal system	Triclinic	Monoclinic
Space group	$P\bar{1}$	$P2_1/c$
a(Å)	7.3139(7)	9.2837(6)
b(Å)	9.6308(9)	25.2187(17)
c(Å)	11.2039(10)	7.4546(5)
α(deg)	73.572(2)	90
β(deg)	78.457(2)	95.4780(10)
γ(deg)	73.711(2)	90
V(Å^3)	720.31(12)	1737.3(2)
Z	1	2
D_{calc}(Mg m^{-3})	2.178	1.871
Crystal size(mm)	0.30 × 0.25 × 0.18	0.45 × 0.39 × 0.28
F(000)	454	948
μ(Mo–Kα) mm^{-1}	5.723	4.739
θ(deg)	1.91 to 25.00	2.20 to 27.88
Reflections collected	3728	10864
Independent reflections	2523 (2461)	4053 (2560)
Parameters	261	259
R_{int}	0.0176	0.0380
$\Delta(\rho)$(e Å^{-3})	0.975 and -1.556	1.107 and -0.926
Goodness of fit	1.068	1.009
R^a	0.0271 (0.0294)[b]	0.0310 (0.0671)[b]
wR_2[a]	0.0571 (0.0582)[b]	0.0589 (0.0670)[b]

* [a] $R = \Sigma||F_o| - |F_c||/\Sigma|F_o|$, w$R_2 = [\Sigma w(F_o^2 - F_c^2)^2/\Sigma w(F_o^2)^2]^{1/2}$; $|F_o| > 4\sigma(|F_o|)$. [b] Based on all data.

Thermal properties.

To examine the thermal stability of the compounds, thermogravimetric analysis (TG) was carried out. And the thermalgravimetric curves of compounds **1** and **2** are shown in Figure S4. For **1**, the first loss-weight is observed at 30 °C and completed at 320 °C, which is in good agreement with the loss of two lattice water molecules (obs:2.22%, calcd:3.81%). The second loss-weight is observed at 321 °C and completes at 710 °C, which is in good agreement with the decomposition of the two chelating carboxyl groups (obs: 11.91%; calcd: 9.32%). The final remaining weight is 86.1%, which is in good responding to the formation of U_3O_8 (calcd 89.1%). And the thermogravimetric curve of compound **2** exhibited that a different weight loss process, compared with **1**, there is no lattice water molecule in compound **2**, the first loss-weight is observed at 114°C and completed at 505 °C, which can be attributed to the loss of uranium metals connected with atriazine rings (obs: 27.25%; calcd: 27.38%). From then on, as the temperature increases, the skeleton continues to furthermore collapse. The final remaining is that UO_3 with carbon residue (obs: 48.12%; calcd: 46.39%).

PXRD analysis.

In order to confirm whether the crystal structures were truly representative of the bulk materials, the PXRD patterns of the compounds **1** and **2** were recorded, as shown in the Figure S5. Compared with the corresponding simulated single-crystal diffraction data, all the peaks present in the measured patterns closely match in the simulated patterns generated from single crystal diffraction data, which indicates that **1** and **2** are in pure phases.

UV-vis Spectroscopy.

The diffuse reflectance UV-vis spectra of compounds **1** and **2** are shown in the Figure S6. Compounds **1** and **2** all presented four peaks, and for **1**, the three absorption peaks appearing at about 211, 262 and 323 nm are associated with the π→π* transition of the ligand, which are similar to the absorbance spectra of the corresponding ligands (H_2L_1 and HL_2), (for **2**, the three absorption peaks appearing at about 215, 265 and 338 nm). And the characteristic equatorial U – O charge transfer band and axial U-O charge transfer band (vibrative coupling) are observed around 429 nm for both compounds **1** and **2**. In addition, according to UV spectra of the compounds, we calculated the band gap of the ligands (H_2L_1 and HL_2) and the two compounds (Figure S7). The values are 3.14, 3.29, 2.98, 2.89 eV, respectively. From these data, we can see that the band gaps of the ligands are bigger than that of theirs corresponding compound, which show furthermore the existence of electronic transitions from the ligand to the metal.

Photoluminescent (PL) properties and nitroaromatics detections.

The fluorescence of inorganic–organic compounds has been currently drawing significant attention in the development of fluorescent materials. The luminescent properties of U^{VI} are of interest due to potential applications including photocatalysis. The utilization of $[UO_2]^{2+}$ ions in compounds arranges the metal centers into an extended topology as well as allows for the introduction of chromophoric organic linkers, which could sensitize the $[UO_2]^{2+}$ luminescence. As we known, the luminescence of uranyl compounds was at near 520 nm. However, not all uranyl compounds possess luminescent properties, and the mechanisms of the emission from uranyl compounds are most often difficult to explain. As shown in the Figure 3a, we can see that compound 1 (λ_{ex} = 351 nm) has a five-peak spectrum, and the five-peak spectrum has been red-shift, compared with the fluorescent of the benchmark compound $UO_2(CH_3COO)_2{\cdot}2H_2O$ (λ_{ex} = 420 nm). Five peaks 482, 495, 517, 541 and 567 nm) for **1** and five peaks (475, 490, 511,

View Article Online
DOI: 10.1039/C6NJ03933B

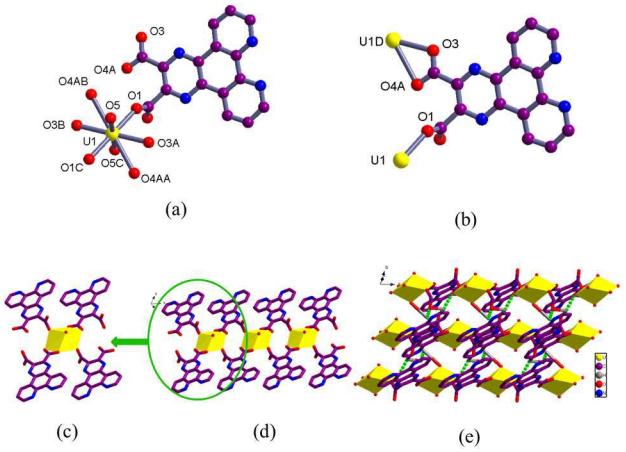

Figure 1. For **1**, (a) Perspective view of the coordination environment around the uranium atom, symmetry codes: A, -1+x, y, z; B, 1-x, 1-y, -z; C, -x, 1-y, -z. (b) Coordination schematic diagram of ligand, symmetry codes: D, 1+x, y, z. (c) The building block of compound **1** formed by four $H_1L_1^-$ ligands and one uranyl bipyramidal polyhedron. (d) The one-dimensional chain structure of compound **1**. (e) The 2D structure of the **1**. Some hydrogen atoms and solvent molecules are omitted for clarity.

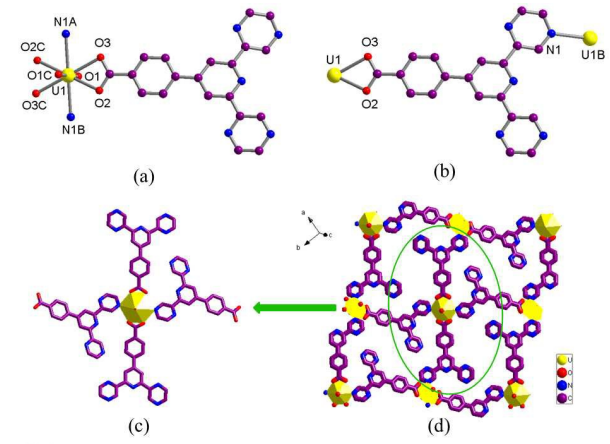

Figure 2. For **2**, (a) Perspective view of the coordination environment around the uranium atom, symmetry codes: A, 1+x, 0.5-y, -0.5+z; B, 2-x, -0.5+y, 0.5-z; C, 3-x, -y,-z. (b) Coordination schematic diagram of ligand, symmetry codes: B, 2-x, -0.5+y, 0.5-z. (c) The building blocks linked with four ligands. (d) The 2D structure of the **2**. Hydrogen atoms and solvent molecules are omitted for clarity.

535 and 561 nm) for $UO_2(CH_3COO)_2{\cdot}2H_2O$, are observed in the spectra, which all exhibit characterized emission from uranyl cations. And the emission peak of 364 nm is from the ligand (H_2L_1) in the compound **1**. For **2**, due to the conjugative ligand H_1L_2, it exhibits strong a broad emission peak at 398 nm (λ_{ex} = 290 nm), which is assigned to the π*→n or π*→π transition (Figure 3b), compared with the fluorescent of the ligand H_1L_2(λ_{ex} = 290 nm). And, another obvious emission peak is at 516 nm, which can be alleged the absorption peak of the uranyl cations, which may be attributed to change electron cloud intensity of the central ring due to coordination with metals.

Based on characterized emission information from uranyl cations, we explored the potential sensing ability of **1** and **2** to sense a trace amount of nitroaromatics; luminescence quenching titrations were

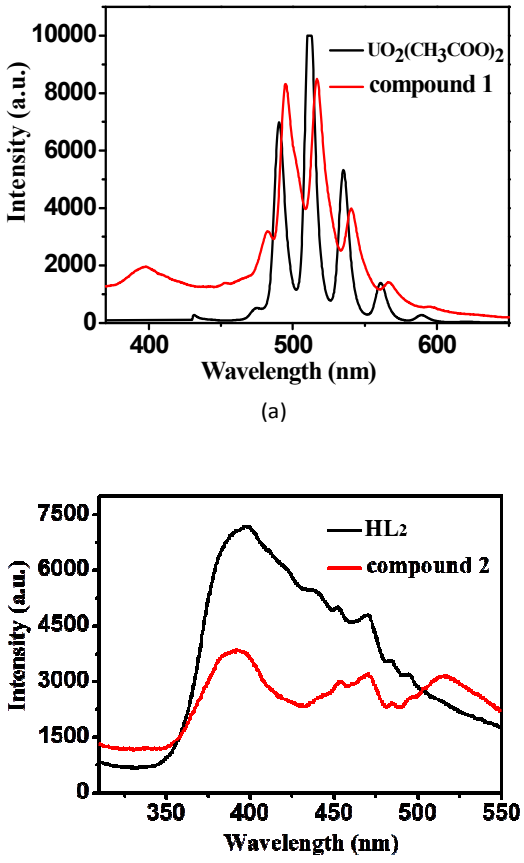

Figure 3. (a) Luminescent spectra of $UO_2(CH_3COO)_2{\cdot}2H_2O$($\lambda_{ex}$ = 420 nm), and compound **1**(λ_{ex} = 351 nm) in the solid state; (b) Luminescent spectra of the ligand H_1L_2(λ_{ex} = 290 nm), and compound **2**(λ_{ex} = 290 nm) in the solid state.

View Article Online
DOI: 10.1039/C6NJ03933B

performed with an incremental addition of nitroaromatics to the compounds **1** and **2** dispersed in the deionized water. First, we clean the compounds, dry, and making them grinded good. Then, taking 2 mg from grinding samples **1** and **2**, respectively, and immersed in the corresponding solvents (3 mL). After treated by ultrasonication for 30 minutes, the samples were suspended in different solvents and change into emulsions. A series of nitroaromatics solvents include 2,4,6-Ttrinitrophenol (TNP), 2,4-dinitrotoluene (DNT), p-Nitroaniline, m-Dinitrobezene, sodium nitrobenzene sulfonate, nitrobenzene (NB) and non-nitro benzene (B). The optimum conditions are at about 25 °C and the solution solubility good, and the solution concentration and solution solubility directly affect the experimental results, so we must control the temperature, concentration, solubility and other issues in the course of the experiment. The two compounds dispersed in deionized water exhibited strong emission in visible region upon excitation at 351 and 290 nm, respectively. To explore the ability of the two compounds to sense a trace amount of nitroaromatics, determination of fluorescence quenching was performed with an incremental addition of nitroaromatics to the two compounds dispersed in deionized water. Here, we take the compound **1** as the main example to research the mechanism of the nitro quenching mechanism, selectivity and sensitivity. As shown in the figure 4a, we can see the changes in the luminescence intensity with the increasing addition of TNP (up to 1000 ppm), and the quenching efficiency is nearly 89% of the initial luminescence intensity for **1**. For **2**, the quenching efficiency is nearly 81%, and luminescence quenching of **2** dispersed in H_2O by gradually increasing TNP concentration was shown in the Figure S8a. Furthermore, in order to determine the detection limit of the TNP, we chose the ultra-low concentrations of TNP to study luminescent response. For **1**, we can see that the fluorescence quenching can still be detected, when the concentration of TNP was as low as 15 ppm, as shown in the Figure 4b. And for **2**, the minimum quenching concentration of TNP is at 20 ppm in the Figure S8b. Similar luminescence quenching was also performed with other nitroaromatics such as 2,4-dinitrotoluene (DNT), p-Nitroaniline, m-Dinitrobezene, sodium nitrobenzene sulfonate, nitrobenzene (NB) and benzene (B) (Figure S9a-f for **1** and Figure S10a-f for **2**). Among these, we found that show the similar luminescence quenching behaviour comparable to the TNP except the benzene (Figure 5 and Figure S11). These results indicate that both the two compounds are effective detectors for nitroaromatics. In the whole testing process, the experimental method is relatively simple and fast, the amount of solution required is relatively small, test time for each sample is about 30s, which can save our time.

To understand the sensitivity and selectivity, the Stern–Volmer plots were used to calculate the quenching constants of the nitroaromatics (Figure 6a and Figure S12a) using the SV equation $(I_0/I) = K_{SV}[A] + 1$, where I_0 and I are the luminescence intensities before and after the addition of the nitroaromatics, [Q] is the molar concentration of the nitroaromatics, and K_{SV} is the quenching constant.[26,27] Different quenchers have varying degrees of impact on the compounds are shown in the Figure 6b and Figure S12b. And as shown in the Table 2, we can see that the K_{SV} values of the quencher TNP are largest for both two compounds, indicating their high sensitivity in detecting small amounts of nitro groups in solution compared with most reported compounds, and the observed K_{SV} values are large, which showed that the both compounds **1** and **2** have a higher sensitivity.[28] In the Table 3, we chose the TNP and DNT as the better quenchers compared with the relevant literature. From it, we can see that the quenching effect is close, and in the solvent, we choose environmentally friendly and non-toxic water as the solvent. From the comparison of K_{SV} values, we can see that the both two compounds have better sensitivity and selectivity. Moreover, we take 50ppm suspension with different quenchers, which mixing compound **1** or **2**, respectively, then, and UV absorption were tested by UV spectra after the centrifugation. As shown in the Figure 7, we can see that the highest UV absorption is TNP for **1** (for **2**, UV absorption is shown in the Figure S13). And as shown in the Figure 8, there is some overlap between the absorption spectra of quenchers and the compounds, and different degree of overlap may also explain why the different quenchers quenching effect are different.

What's more, the homogeneous dispersible nature of the submicron sized uranium–organic materials has enabled a close contact between the compounds and the nitroaromatics. The most important factor of the dynamic quenching maybe due to that the nitroaromatics with electron-deficient property can obtain an electron from excited state of the ligand. In other words, the excited state electrons can transfer from UOFs to nitroaromatics, which lead to luminescence quenching.[30] And the nitroaromatics with electron-deficient can obtain an electron from excited state of the ligand, which has been confirmed by molecular orbital theory. The LUMO of nitroaromatics is a low-lying π*-type orbital stabilized by -NO_2 through conjugation effect, so it should be lower than LUMO of the ligand, which can also explain the mechanism of nitro-quenched.[31] And as we known, electron-transfer or energy transfer between the compounds and the quenchers account for the fluorescence quenching of the compounds. So, the main quenching mechanism for quenchers may be an excited state charge transfer between the excited state of the compounds and the ground state of the quenchers.[32]

Aldehydes detections.

In addition, we studied the fluorescence response of compound **2** towards to formaldehyde and benzaldehyde molecules at ultra-low concentrations, the experimental methods are similar to the fluorescence test methods of compounds towards to nitroaromatics. Taking **2** mg from grinding sample **2** and then immersed in the corresponding concentration of the ethanol solution (3 mL). After treated by ultrasonication for 30 minutes, the samples were completely dissolved. The compound **2** dispersed in ethanol exhibited strong emission in visible region upon excitation at 290 nm. As shown in the Figure 9, we could see that with the increase of the concentration of the aldehyde, the fluorescence intensity is also enhanced. This showed a turn-on fluorescence responsive behavior, which may be interpreted as the ligand and aldehyde to form a π*-π conjugation, and the π*-π conjugation work synergistically to impede the rotation-induced energy dissipation, and making the rigid skeleton strengthened, so the fluorescence enhanced.[33]

View Article Online
DOI: 10.1039/C6NJ03933B

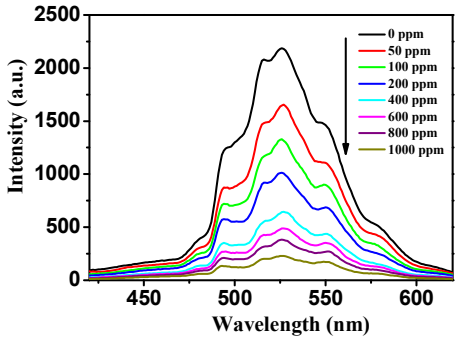

(a)

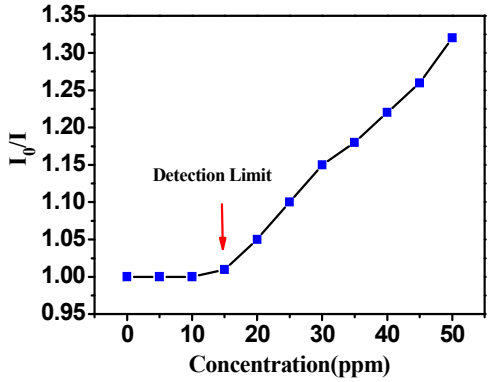

(b)

Figure 4. (a) Luminescence quenching of **1** dispersed in H_2O by gradually increasing TNP concentration; (b) the detection limit of TNP for **1**.

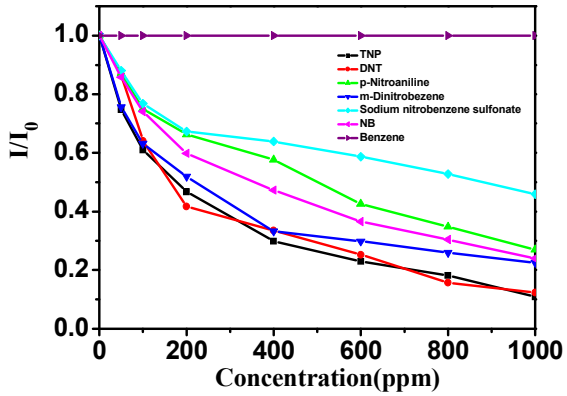

Figure 5. Plot of fraction of luminescence intensity of **1** vs. concentration of analytes, I_0 and I are the luminescence intensities in the absence and presence of nitroaromatics, respectively.

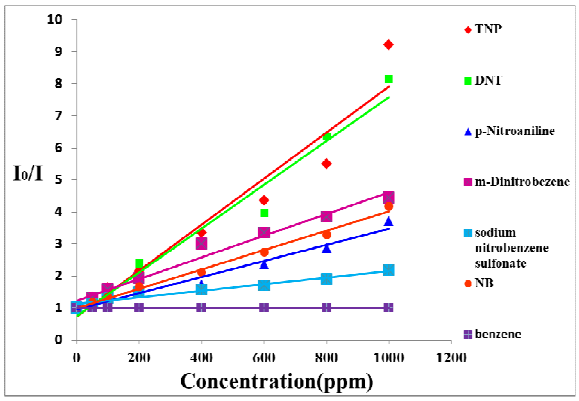

(a)

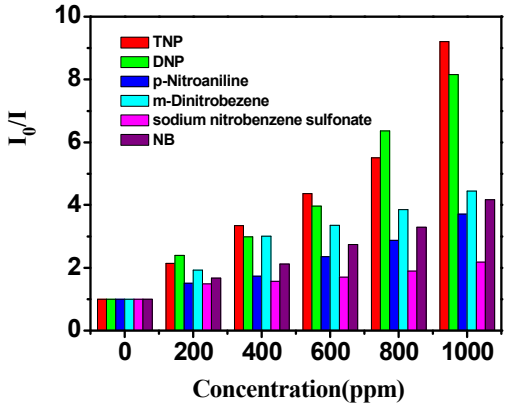

(b)

Figure 6. For **1**, (a) linear relationships of the quenching are fluorescence intensity ratio and quencher concentration; (b) at different concentrations, the value of the fluorescence intensities and the quencher ratios.

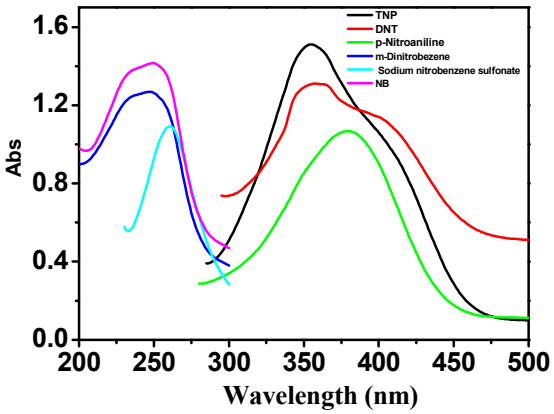

Figure 7. UV absorption of different quenchers with compound **1:** TNP, DNT, p-Nitroaniline, m-Dinitrobezene, Sodium nitrobenzene sulfonate and NB, respectively.

View Article Online
DOI: 10.1039/C6NJ03933B

Table 2. Different quenchers' K_{SV} of the compounds **1** and **2**.

Analyte	**1** [K_{SV}(M^{-1})]	**2** [K_{SV}(M^{-1})]
TNP	1.6×10^{6}	8.5×10^{5}
DNT	1.3×10^{6}	3.9×10^{5}
m-Dinitrobezene	7.4×10^{5}	4.1×10^{5}
NB	3.7×10^{5}	4.8×10^{5}
p-Nitroaniline	3.5×10^{5}	4.4×10^{5}
sodium nitrobenzene sulfonate	2.3×10^{5}	3.6×10^{5}

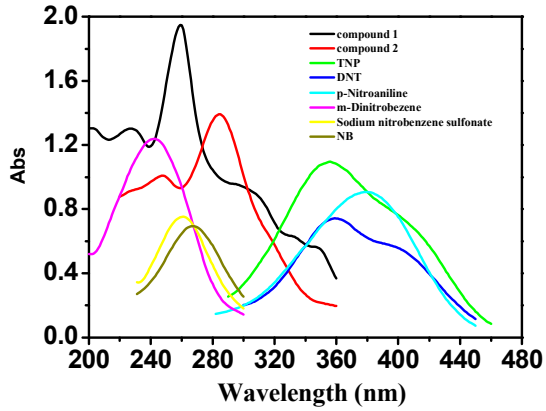

Figure 8. UV absorption of two compounds and different quenchers.

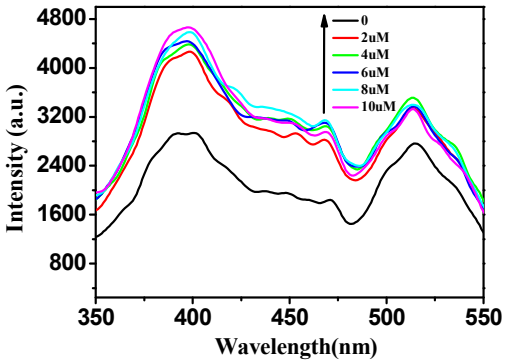

(a)

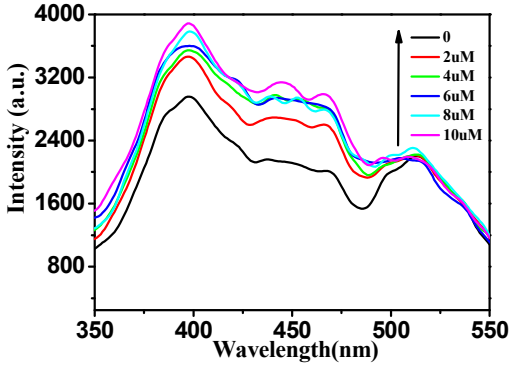

(b)

Figure 9. (a) Luminescence enhancement of **2** dispersed in ehanol by gradually increasing formaldehyde concentration; (b) Luminescence enhancement of **2** dispersed in ehanol by gradually increasing benzaldehyde concentration.

Table 3. Comparison of data about different compounds for the detection of nitroaromatics.

Quenchers	Compounds	*Ksv*'s value(M^{-1})	Quenching efficiency(%)	Solvent	References
TNP	The guest free Tb@1 (Tb@1')	7.09×10^{4}	96	acetonitrile	12
	$[Cd_4(\mu_3\text{-}O)(TTHA)(H_2O)_2]\cdot3H_2O$	3.83×10^{4}	97	H_2O	27
	$UO_2(HL_1)_2\cdot2H_2O$ (**1**)	1.6×10^{6}	89	H_2O	This work
	$UO_2(L_2)_2$ (**2**)	8.5×10^{5}	81	H_2O	This work
DNT	[Cd(HL1)(L2)]	-	-	DMF	29
	$[Cd_4(\mu_3\text{-}O)(TTHA)(H_2O)_2]\cdot3H_2O$	-	-	H_2O	27
	$UO_2(HL_1)_2\cdot2H_2O$ (**1**)	1.3×10^{6}	87	H_2O	This work
	$UO_2(L_2)_2$ (**2**)	3.9×10^{5}	86	H_2O	This work

View Article Online
DOI: 10.1039/C6NJ03933B

Conclusions

In this work, we have successfully synthesized two new compounds, $UO_2(C_{16}H_7N_4O_4)_2{\cdot}2H_2O$ (**1**) and $UO_2(C_{20}H_{12}N_5O_2)_2$ (**2**), under the hydrothermal condition by using different heterocyclic carboxyl ligands, 2,3-pyrazino[1,10]phenanthroline-2,3dicarboxylic acid (H_2L_1) and 2,6-bis(2-pyrazinyl)pyridine-4-benzoic acid (HL_2). By the single crystal analysis, both compounds **1** and **2** exhibited a 2D sheet structure. The luminescence studies reveal that compounds **1** and **2** display selectivity and sensitivity to nitroaromatics in deionized water. The results show that **1** and **2** may be used for nitroaromatics sensing application. In addition, compound **2** showed a turn-on fluorescence responsive behavior towards to aldehyde compounds. In summary, the successful syntheses of the two compounds and the finding of their unusual physicochemical properties may also help to explore new types of sensing materials and detect the trace of explosive materials.

Acknowledgements

We are grateful for support provided by the National Natural Science Foundation of China (Grant Nos. 21571091, 21371086), Guangxi Key Laboratory of Information Materials, Guilin University of Electronic Technology, P. R. China (Grant No. 151002-K), and State Key Laboratory of Inorganic Synthesis and Preparative Chemistry, College of Chemistry, Jilin University, Changchun 130012, P.R. China (Grant No. 2016-02).

Notes and references

1 (a) W. C. Trogler, *NATO ASI Workshop, Electronic Noses & Sensors for the Detection of Explosives,* ed. J. W. Gardner and J. Yinon, Kluwer Academic Publishers, Dordrecht, The Netherlands, 2004; (b) B. Gole, A. K. Bar and P. S. Mukherjee, *Chem.Eur. J.,* 2014, **20**, 2276.
2 D. K. Singha, P. Majee, S. K. Mondal and P. Mahata, *RSC Adv.,* 2015, **5**, 102076.
3 (a) S. R. Zhang, D. Y. Du, J. S. Qin, S. J. Bao, S. L. Li, W. W. He, Y. Q. Lan, P. Shen and Z. M. Su, *Chem. Eur. J.,* 2014, **20**, 3589; (b) S. J. Toal and W. C. Trogler, *J. Mater. Chem.,* 2006, **16**, 2871; (c) Y. Salinas, R. Martinez- Manez, M. D. Marcos, F. Sancenon, A. M. Costero, M. Parra and S. Gil, *Chem. Soc. Rev.,* 2012, **41**, 1261.
4 D. K. Singha and P. Mahata, *RSC Adv.,* 2015, **5**, 28092.
5 S. W. Thomas III, G. D. Joly and T. M. Swager, *Chem. Rev.,* 2007, **107**, 1339.
6 (a) S. Sarkar, S. Dutta, S. Chakrabarti, P. Bairi and T. Pal, *ACS Appl. Mater. Interfaces,* 2014, **6**, 6308; (b) Y. Salinas, R. Martinez-Manez, M. D. Marcos, F. Sancenon, A. M. Costero, M. Parra and S. Gil, *Chem. Soc. Rev.,* 2012, **41**, 1261.
7 Y. L. Wang, Z. Y. Liu, Y. X. Li, Z. L. Bai, W. Liu, Y. X. Wang, X. M. Xu, C. L. Xiao, D. P. Sheng, J. Diwu, J. Su, Z. F. Chai, T. E. Albrecht-Schmitt and S. A. Wang, *J. Am. Chem. Soc.*,2015,**137(19)**, 6144.
8 (a) S. S. Nagarkar, A. V. Desai and S. K. Ghosh, *Chem. Commun.,* 2014, **50**, 8915; (b) D. K. Singha, P. Majee, S. K. Mondal and P. Mahata, *Eur. J. Inorg. Chem.,* 2015, 1390.
9 S. W. Thomas, G. D. Joly and T. M. Swager, *Chem. Soc. Rev.,* 2007, **36**, 1339.
10 B. Gole, A. K. Bar, and P. S. Mukherjee, *Chem. Eur. J.,* 2014, **20**, 13321.
11 (a) S. S. Nagarkar, A. V. Desai and S. Ghosh, *Chem. Commun.,* 2014, **50**, 8915; (b) G. He, H. Peng, T. Liu, M. Yang, Y. Zhang and Y. Fang, *J. Mater. Chem.,* 2009, **19**, 7347.
12 D. K. Singha, S. Bhattacharya, P. Majee, S. K. Mondal,M. Kumar and P. Mahata, *J. Mater. Chem. A,* 2014, **2**, 20908.
13 B. Roy, A. K. Bar, B. Gole and P. S. Mukherjee, *J. Org. Chem.,* 2013, **78**, 1306.
14 (a) D. S. Moore, *Rev. Sci. Instrum.,* 2004, **75**, 2499; (b) G. E. Spangler, J. P. Carrico, and D. N. Campbell, *J. Test. Eval.,* 1985, **13**, 234; (c) L. M. Dorozhkin, V. A. Nefedov, A. G. Sabelnikov, and V. G. Sevastjanov, *Sens. Actuators B,* 2004, **99**, 568; (d) E. S. Forzani, D. L. Lu, M. J. Leright, A. D. Aguilar, F. Tsow, R. A. Iglesias, Q. Zhang, J. Lu, J. H. Li, and N. J. Tao, *J. Am. Chem. Soc.,* 2009, **131**, 1390; (e) R. A. McGill, T. E. Mlsna, R. Chung, V. K. Nguyen, and J. Stepnowski, *Sens. Actuators B,* 2000, **65**, 5.
15 (a) D. Li, J. Liu, R. T. K. Kwok, Z. Liang, B. Z. Tang and J. Yu, *Chem. Commun.,* 2012, **48**, 7167; (b) E. S. Snow, F. K. Perkins, E. J. Houser, S. C. Badescu and T. L. Reinecke, *Science*, 2005, **307**, 1942; (c) B. Gole, S. Shanmugaraju, A. K. Bar and P. S. Mukherjee, *Chem. Commun.,* 2011, **47**, 10046; (d) S. Shanmugaraju, S. A. Joshi and P. S. Mukherjee, *Inorg. Chem.,* 2011, **50**, 11736; (e) K. K. Kartha, S. S. Babu, S. Srinivasan and A. Ajayaghosh, *J. Am. Chem. Soc.,* 2012, **134**, 4834.
16 W. Liu, L. J. Liu, Y. L. Wang, L. H. Chen, J. A. McLeod, L. J. Yang, J. Zhao, Z. Y. Liu, J. Diwu, Z. F. Chai, T. E. Albrecht-Schmitt, G. K. Liu, and S. A. Wang, *Chemistry-A European Journal*, 2016, **22**, 11170.
17 (a) T. Y. Shvareva, P. M. Almond, and T. E. Albrecht-Schmitt, *J. Solid State Chem.,* 2005, **178**, 499; (b) T. Y. Shvareva, T. A. Sullens, T. C. Shehee, and T. E. Albrecht-Schmitt, *Inorg. Chem.,* 2005, **44**, 300; (c) K. M. Ok, J. Baek, and P. S. Halasyamani, *Inorg. Chem.,* 2006, **45**, 10207; (d) D. Grohol, and E. L. Blinn, *Inorg. Chem.,* 1997, **36**, 3422.
18 (a) M. Frisch, and C. L. Cahill, *Dalton Trans.,* 2006, **39**, 4679; (b) C. L. Cahill, D. T. de Lill, and M. Frisch, *CrystEngComm.,* 2007, **9**, 15.
19 (a) R. E. Sykora, J. E. King, A. J. Illies, and T. E. Albrecht-Schmitt, *J. Solid State Chem.,* 2004, **117**, 1717; (b) Z. L. Liao, G. D. Li, M. H. Bi, and J. S. Chen, *Inorg. Chem.,* 2008, **47**, 4844; (c) Z. T. Yu, Z. L. Liao, Y. S. Jiang, G. H. Li, and J. S. Chen, *Chem. Eur. J.,* 2005, **11**, 2642-2650; (d) X. T. Xu, Y. N. Hou, S. Y. Wei, X. X. Zhang, F. Y. Bai, L. X. Sun, Z. Shi, and Y. H. Xing, *CrystEngComm.,* 2015, **17**, 642.
20 (a) J. L. Sessler, P. J.Melfi, and G. D. Pantos, *Coord. Chem. Rev.,* 2006, **250**, 816; (b) M. B. Jones, and A. J. Gaunt, *Chem. Rev.,* 2013, **113**, 1137; (c) I. Mihalcea, C. Volkringer, N. Henry, and T. Loiseau, *Inorg. Chem.,* 2012, **51**, 9610; (d) J. W. Napoline, S. J. Kraft, E. M. Matson, P. E. Fanwick, S. C. Bart, and C. M. Thomas, *Inorg. Chem.,* 2013, **52**, 12170; (e) T. Loiseau, I. Mihalcea, N. Henry, and C. Volkringer, *Coord. Chem. Rev.,* 2014, **266-267**, 69.
21 (a) M. B. Andrews and C. L. Cahill, *Chem. Rev.,* 2013, **113**, 1121-1136; (b) J. Qiu and P. C. Burns, *Chem. Rev.,* 2013, **113**, 1097; (c) P. Thuéry, Cryst. *Growth Des.,* 2010, **10**, 2061; (d) Y. X. Li, Z. H. Weng, Y. L. Wang, L. H. Chen, D. P. Sheng, J. Diwu, Z. F. Chai, T. E. Albrecht-Schmitt and S. A. Wang, *Dalton Trans.*, 2016, **45**, 918.
22 A. Stublla and P. G. Potvin, *Eur. J. Inorg. Chem.,* 2010, 3040–3050.
23 G. M. Sheldrick, SADABS, Program for Empirical Absorption Correction for area Detector Data; University of Gottingen: Gottingen, Germany, 1996.
24 G. M. Sheldrick, SHELXS 97, Program for Crystal Structure Refinement; University of Gottingen: Gottingen, Germany, 1997.

View Article Online
DOI: 10.1039/C6NJ03933B

25 (a) B. Masci and P. Thuéry, *Cryst. Growth Des.,* 2008, **8**, 1689-1696; (b) P. Thuéry, *Cryst. Growth Des.,* 2011, **11**, 2606-2620.
26 (a) D. K. Singha, S. Bhattacharya, P. Majee, S. K. Mondal, M. Kumara and P. Mahata，*J. Mater. Chem. A,* 2014, **2**, 20908; (b) D. K. Singha and P. Mahata, *RSC Adv.,* 2015, **5**, 28092; (c) K. Acharyya and P. S. Mukherjee, *Chem. Eur. J.,* 2015, **21**, 6823; (d) B. Gole, A. K. Bar, and P. S. Mukherjee, *Chem. Eur. J.,* 2014, **20**, 13321; (e) S. Shanmugaraju and P. S. Mukherjee, *Chem. Eur. J.,* 2015, **21**, 6656; (f) B. Gole, W. Song, M. Lackinger, and P.S.Mukherjee, *Chem. Eur. J.,* 2014, **20**, 13662 .
27 S. Li, J. Song, J. C. Ni, Z. N. Wang, X.Gao, Z. Shi, F. Y. Bai and Y. H. Xing, *RSC Adv.,* 2016, **6**, 36000
28 M. Guo and Z. M. Sun, *J. Mater. Chem.,* 2012, **22**, 15939.
29 L. Lu, J.Wang, W. P Wu, A. Q. Ma, J. Q. Liu, R. Yadav, A. Kumar, Journal of Luminescence, dx.doi.org/10.1016/j.jlumin.2017.02.010.
30 (a) S. Dang, X. Min, W. Yang, F. Y. Yi, H. You, and Z. M. Sun, *Chem. Eur. J.,* 2013, **19**, 17172; (b) S. S. Nagrkar, B. Joarder, A.K. Chaudhari, S. Mukherjee, and S. K. Ghosh, *Angew. Chem., Int. Ed.,* 2013, **52**, 2881; (c) X. Zhou, H. Li, H. Xiao, L. Li, Q. Zhao, T. Yang, J. Zuo and W. Huang, *Dalton Trans.,* 2013, **42**, 5718; (d) S. Pramanik, Z. Hu, X. Zhang, C. Zheng, S. Kelly and J. Li, *Chem. Eur. J.,* 2013, **19**, 15964; (e) G. Y. Wang, C. Song, D. M. Kong, W. J. Ruan, Z. Chang and Y. Li, *J. Mater. Chem. A,* 2014, **2**, 2213; (f) J. S. Qin, S. J. Bao, P. Li, W. Xie, D. Y. Du, L. Zhao, Y. Q. Lan and Z. M. Su, *Chem. Asian J.,* 2014, **9**, 749.
31 (a) Y. C. He, H. M. Zhang, Y. Y. Liu, Q. Y. Zhai, Q. T. Shen, S. Y. Song and J. F. Ma, Cryst. Growth Des., 2014, 14, 3174; (b) D. Tian, Y. Li, R. Y. Chen, Z. Chang, G. Y. Wang and X. H. Bu, J. Mater. Chem. A, 2014, 2, 1465.
32 E. Wang, D. M. Sun, H. H. Li, X. L. Sun, J. T. Liu, Z. J. Ren and S. K. Yan, *J. Mater. Chem.*, 2016, **4**, 6756.
33 S. Dalapati, E. Jin, M. Addicoat, T. Heine,and D. Jiang, *J. Am. Chem. Soc.* 2016, **138**, 5797.

View Article Online
DOI: 10.1039/C6NJ03933B

Two Uranyl Heterocyclic Carboxyl Compounds with Fluorescent Properties as High Sensitivity and Selectivity Optical Detectors for Nitroaromatics

Shuang Li,[a] Li Xian Sun,[b] Jue Chen Ni,[a] Zhan Shi,[c] Yong Heng Xing,*[a] Di Shang,[a] Feng Ying Bai*[a]

[a] College of Chemistry and Chemical Engineering, Liaoning Normal University, Dalian City, 116029, China. E-mail: xingyongheng2000@163.com, baifengying2000@163.com

[b] Guangxi Key Laboratory of Information Materials, Guilin University of Electronic Technology, Guilin 541004, P.R. China.

[c] State Key Laboratory of Inorganic Synthesis and Preparative Chemistry, College of Chemistry, Jilin University, Changchun 130012, P.R. China

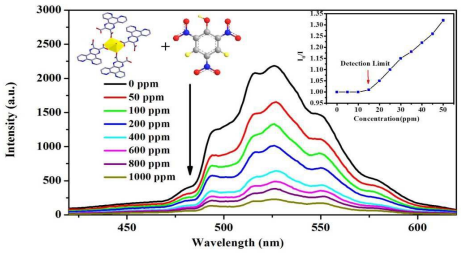

Uranyl skeleton compounds showed strong sensitivity and selectivity for the detection of nitroaromatic.